Get More with SINTA Insight

Go to Insight

INTERNATIONAL JOURNAL OF APPLIED SCIENCES AND SMART TECHNOLOGIES

UNIVERSITAS SANATA DHARMA

P-ISSN : 26558564 E-ISSN : 26859432

0.857143
Impact Factor

138
Google Citations

Sinta 4
Current Acreditation

Google Scholar Garuda Website Editor URL

History Accreditation

2020 2021 2022 2023 2024

Garuda Google Scholar

[Forensic Investigation in SQL Server Database Using Temporal Tables & Extended Events Artifacts]

Universitas Sanata Dharma International Journal of Applied Sciences and Smart Technologies
Volume 05, Issue 01, June 2023 1 - 16
2023 DOI: 10.24071/ijasst.v5i1.4611 Accred : Sinta 4

[Smoothing Module for Optimization Cranium Segmentation Using 3D Slicer]

Universitas Sanata Dharma International Journal of Applied Sciences and Smart Technologies
Volume 05, Issue 01, June 2023 75 - 88
2023 DOI: 10.24071/ijasst.v5i1.6300 Accred : Sinta 4

[Rfid Application For Designing Lowcost Learning Device For Play And Learning To Read Early Braille For Blind Children]

Universitas Sanata Dharma International Journal of Applied Sciences and Smart Technologies
Volume 05, Issue 01, June 2023 17 - 26
2023 DOI: 10.24071/ijasst.v5i1.5599 Accred : Sinta 4

[A Brief on Optical-based Investigation towards The Interfacial Behaviors during High Viscous Liquid/Gas Countercurrent Two-Phase Flow in a Complex Conduit Representing 1/30 Down-Scaled of PWR Hot Leg Geometry]

Universitas Sanata Dharma International Journal of Applied Sciences and Smart Technologies
Volume 05, Issue 01, June 2023 101 - 112
2023 DOI: 10.24071/ijasst.v5i1.6302 Accred : Sinta 4

[Smart Technology in Construction Industry: Opportunity during COVID-19 Pandemic]

Universitas Sanata Dharma International Journal of Applied Sciences and Smart Technologies
Volume 05, Issue 01, June 2023 27 - 38
2023 DOI: 10.24071/ijasst.v5i1.5583 Accred : Sinta 4

[Performance of Low Power Electric Energy Clothes Dryers for Households]

Citation Per Year By Google Scholar

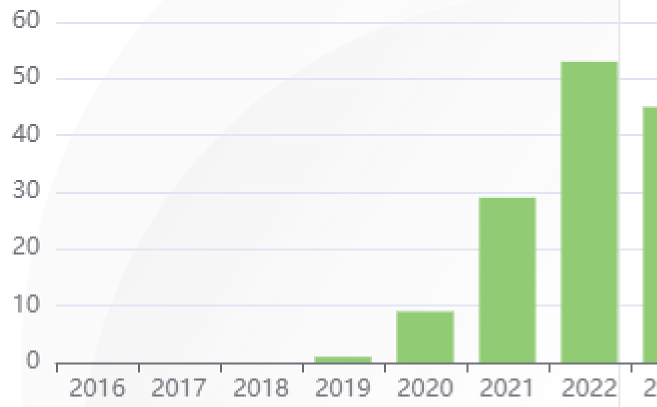

Journal By Google Scholar

	All	Since 2019
Citation	138	138
h-index	5	5
i10-index	3	3

Universitas Sanata Dharma International Journal of Applied Sciences and Smart Technologies
Volume 05, Issue 01, June 2023 39 - 54
2023 DOI: 10.24071/ijasst.v5i1.6281 Accred : Sinta 4

Application of Augmented Reality-Based Solar System Recognition Using Metaverse Studio
Universitas Sanata Dharma International Journal of Applied Sciences and Smart Technologies
Volume 05, Issue 01, June 2023 55 -66
2023 DOI: 10.24071/ijasst.v5i1.5447 Accred : Sinta 4

Input Power Measurement System for Driving Motor in Testing Low-Speed Generator
Universitas Sanata Dharma International Journal of Applied Sciences and Smart Technologies
Volume 05, Issue 01, June 2023 113 - 132
2023 DOI: 10.24071/ijasst.v5i1.6339 Accred : Sinta 4

Laser Based Vibration Sensor Through Mobile
Universitas Sanata Dharma International Journal of Applied Sciences and Smart Technologies
Volume 05, Issue 01, June 2023 67 - 74
2023 DOI: 10.24071/ijasst.v5i1.4695 Accred : Sinta 4

Classification of Lung and Colon Cancer Histopathological Images Using Convolutional Neural Network (CNN) Method on a Pre-Trained Models
Universitas Sanata Dharma International Journal of Applied Sciences and Smart Technologies
Volume 05, Issue 01, June 2023 133 - 142
2023 DOI: 10.24071/ijasst.v5i1.6325 Accred : Sinta 4

View more ...

Citation Per Year By Google Scholar

Journal By Google Scholar

	All	Since 2019
Citation	138	138
h-index	5	5
i10-index	3	3

International Journal of Applied Sciences and Smart Technologies

p-ISSN : 2655 - 8564
e-ISSN : 2685 - 9432

International Journal of Applied Sciences and Smart Technologies

International Journal of Applied Sciences and Smart Technologies (IJASST) is published by Faculty of Science and Technology, Sanata Dharma University Yogyakarta-Central Java-Indonesia. IJASST is an open-access peer reviewed journal that mediates the dissemination of academicians, researchers, and practitioners in engineering, science, technology, and basic sciences which relate to technology including applied mathematics, physics, and chemistry. IJASST accepts submission from all over the world, especially from Indonesia

Announcements

National Accreditation for IJASST

IJASST has been nationally accredited by the Ministry of Research and Technology/National Research and Innovation Agency of the Republic of Indonesia (**Volume 2 No 1 2020 - Volume 6 No 2 2024**) and indexed in **SINTA 4.**

Decree No. 204/E/KPT/2022 on October 03rd, 2022

SERTIFIKAT
Direktorat Jenderal Pendidikan Tinggi, Riset dan Teknologi
Kementerian Pendidikan, Kebudayaan, Riset dan Teknologi Republik Indonesia
Kutipan dari Keputusan Direktorat Jenderal Pendidikan Tinggi, Riset dan Teknologi Kementerian Pendidikan, Kebudayaan, Riset, dan Teknologi Republik Indonesia
Nomor 204/E/KPT/2022
Peringkat Akreditasi Jurnal Ilmiah periode II Tahun 2022
Nama Jurnal Ilmiah
International Journal of Applied Sciences and Smart Technologies
E-ISSN: 26859432
Penerbit: Universitas Sanata Dharma
Ditetapkan Sebagai Jurnal Ilmiah
TERAKREDITASI PERINGKAT 4
Akreditasi Berlaku selama 5 (lima) Tahun, yaitu Volume 2 nomor 1 tahun 2020 sampai volume 6 nomor 2 tahun 2024
Jakarta, 03 October 2022
Plt. Direktur Jenderal Pendidikan Tinggi, Riset, dan Teknologi
Prof. Ir. Nizam, M.Sc., DIC, Ph.D., IPU, ASEAN Eng
NIP. 196107061987101001

Posted: 2023-01-02

More Announcements...

Volume 06, Issue 01, June 2024 (In progress)

Volume 06, Issue 01, June 2024 (***In progress***)

Table of Contents

Articles

International Journal of Applied Sciences and Smart Technologies

p-ISSN : 2655 - 8564
e-ISSN : 2685 - 9432

Editorial Team

Publisher : Faculty of Science and Technology

Society/Institution : Sanata Dharma University

International Journal of Applied Sciences and Smart Technologies

p-ISSN : 2655 - 8564
e-ISSN : 2685 - 9432

HOME ABOUT LOGIN REGISTER SEARCH CURRENT ARCHIVES ANNOUNCEMENTS

Home > Archives > **Volume 06, Issue 01, June 2024 (In progress)**

Volume 06, Issue 01, June 2024 (In progress)

DOI: https://doi.org/10.24071/ijasst.v6i1

Volume 06, Issue 01, June 2024 (*In progress*)

Table of Contents

Articles

Publisher : Faculty of Science and Technology

Society/Institution : Sanata Dharma University

OPEN JOURNAL SYSTEMS

Journal Help

USER
Username
Password
Remember me
Login

NOTIFICATIONS
- View
- Subscribe

LANGUAGE
Select Language
English
Submit

JOURNAL CONTENT
Search
Search Scope
All
Search

Browse
- By Issue
- By Author
- By Title
- Other Journals

FONT SIZE

INFORMATION
- For Readers
- For Authors
- For Librarians

Article Template

LaTeX Template

International Journal of Applied Sciences and Smart Technologies

Volume 6, Issue 1, pages 1–9

p-ISSN 2655-8564, e-ISSN 2685-9432

IJASST

Design Of Maximum Torque Per Ampere Control Method In Squirrel Cage Three-Phase Induction Motor

Regina Chelinia Erianda Putri[1, *], Feri Yusivar [2]

[1]*Faculty of Science and Technology, Sanata Dharma University, Yogyakarta, 55281, Indonesia*

[2] *Faculty of Engineering, University of Indonesia, Depok, 16424, Indonesia*

[*]*Corresponding Author: regina.chelinia@usd.ac.id*

(Received 19-10-2023; Revised 06-12-2023; Accepted 10-01-2024)

Abstract

Improving the performance of three-phase induction motors is currently carried out by various control methods. One of them is controlling a three-phase induction motor using the Maximum Torque Per Ampere (MTPA) method. This paper focuses on the study of modeling specific motor models using the MTPA method. The purpose of the study is to prove that with the squirrel cage motor model, the speed can be increased above its rating. The MTPA method is a method of controlling a three-phase induction motor by controlling the current from the torque speed. Modeling is tested to see the responsiveness of the modeled system. The experimental results were tested using two-speed references and the system showed that MTPA control induction motors can improve the performance of three-phase induction motors. The results from the design show that the MTPA method can increase the performance of three-phase induction motors to reach 84.4%. The results of this study can be used as one way to model induction motors.

Keywords: Induction Motor, Modelling, MTPA

1 Introduction

Developments in the field of transportation in the current era are growing rapidly. However, it is not balanced with waste treatment, making the environment polluted with smoke pollution. According to the results of the study "In the last 100 years the earth has increased in temperature up to 0.18 degrees Celsius" [1].

The transition from fossil fuel energy to electrical energy as energy in the field of transportation requires one component of electric vehicle design, namely the induction

Volume 6, Issue 1, pages 1–9
p-ISSN 2655-8564, e-ISSN 2685-9432

motor. A three-phase induction motor is an electronic device that aims to convert electrical energy into mechanical energy. A widely used induction motor is a three-phase induction motor known as an asynchronous motor, called because of the difference in speed from the rotation of the rotor to the rotation speed of the stator.

Such as previous research Direct Quadrate (D-Q) Modeling in the Speed Control System of Three Phase Induction Motors With Field Oriented Control (FOC) Based on P-I Controlled [2] about controlling induction motors with FOC based on PI controllers, and Speed Sensorless Control of Parallel Connected Dual Induction Motor Fed by Single Inverter using Direct Torque Control about controlling two induction motors with parallel induction motors [3]

The purpose of this study is to prove that with certain motorcycle models, speed can be increased above its rating. The MTPA method is a three-phase induction motor control method by adjusting the reference input of torque current and flux current to control the rotational speed of the induction motor. MTPA is designed to ensure that the current used is the minimum i_d current for development at motor torque, with the total stator flux controlled by the MTPA criterion.

2 Research Methodology

The system uses models and methods, namely induction motor models, Clark-Park transformation methods, Rotor Field Oriented Control (RFOC), and MTPA modeling.

A. Induction motor model

Induction motor modeling uses the stator voltage vector $(v_s)'$, the stator current vector $(i_s)'$, the stator flux vector $(\psi_s)'$ and the rotor flux vector $(\psi_r)'$. The general equation of induction motor is as follows

$$\overrightarrow{V_s}' = R_s\overrightarrow{\iota_s}' + \frac{d}{dt}\overrightarrow{\psi_s}' + j\omega_e\overrightarrow{\psi_s} \quad \text{(Eq. 1)}$$

$$\overrightarrow{V_r}' = R_r\overrightarrow{\iota_r}' + \frac{d}{dt}\overrightarrow{\psi_r}' + j(\omega_e - \omega_r)\overrightarrow{\psi_r} \quad \text{(Eq. 2)}$$

$$\overrightarrow{\psi_s}' = L_s\overrightarrow{\iota_s}' + L_m\overrightarrow{\iota_r}' \quad \text{(Eq. 3)}$$

Volume 6, Issue 1, pages 1–9
p-ISSN 2655-8564, e-ISSN 2685-9432

$$\overrightarrow{\psi_r}' = L_r\overrightarrow{\iota_r}' + L_m\overrightarrow{\iota_s}' \qquad \textit{(Eq. 4)}$$

B. Clark-Park Transformation

The induction motor used is a three-phase induction motor, but modeling is carried out in two phases which aims to simplify calculations and analysis. Transformation from three phases to two phases, the transformations used are Clarke Transformation and Park Transformation.

The Clarke transform is a transformation that transforms a system that is on the (abc axis) into a stationary state frame of reference ($\alpha\beta$ axis). In the stator frame of reference, $\omega_e = 0$ and then in the cage rotor type, the terminals are briefly connected so that the rotor voltage is $V_r = 0$. The substitution of the equation of stator current and rotor current obtained induction motor model in the $\alpha\beta$ axis becomes,

$$\frac{d}{dt}i_{s\alpha} = \left(-\frac{R_s}{\sigma L_s} - \frac{(1-\sigma)}{\sigma\tau_r}\right)i_{s\alpha} + \frac{L_m}{\sigma L_s L_r \tau_r}\psi_{r\alpha} + \frac{L_m\omega_r}{\sigma L_s L_r}\psi_{r\beta} + \frac{1}{\sigma L_s}V_{s\alpha} \qquad \textit{(Eq. 5)}$$

$$\frac{d}{dt}i_{s\beta} = \left(-\frac{R_s}{\sigma L_s} - \frac{(1-\sigma)}{\sigma\tau_r}\right)i_{s\beta} - \frac{L_m\omega_r}{\sigma L_s L_r}\psi_{r\alpha} + \frac{L_m}{\sigma L_s \tau_r L_r}\psi_{r\beta} + \frac{1}{\sigma L_s}V_{s\beta} \qquad \textit{(Eq. 6)}$$

$$\frac{d}{dt}\psi_{r\alpha} = \frac{R_r}{L_r}L_m i_{s\alpha} - \frac{R_r}{L_r}\psi_{r\alpha} - \omega_r\psi_{r\beta} \qquad \textit{(Eq. 7)}$$

$$\frac{d}{dt}\psi_{r\beta} = \frac{R_r}{L_r}L_m i_{s\beta} + \omega_r\psi_{r\alpha} - \frac{R_r}{L_r}\psi_{r\beta} \qquad \textit{(Eq. 8)}$$

with $\sigma = \frac{L_s L_r - L_m^2}{L_s L_r}$ and $\tau_r = \frac{L_r}{R_r}$

Park transform is a transformation that transforms a two-phase system that is on a stationary frame of reference (αβ axis) transformed in a rotating frame of reference (dq axis). In the rotor frame of reference the location ω_e is put together by the axis of the rotor causing the magnitude of ω_e is not equal to zero. The stator voltage transformation in equations (1)-(4) will be [4]:

$$\frac{d}{dt}i_{sd} = \left(-\frac{R_s}{\sigma L_s} - \frac{L_m^2}{\sigma L_s L_r \tau_r}\right)i_{sd} + \omega_e i_{sq} + \frac{L_m}{\sigma L_s L_r \tau_r}\psi_{rd} + \frac{L_m}{\sigma L_s L_r}\omega_r\psi_{rq} + \frac{1}{\sigma L_s}V_{sd}) \qquad \textit{(Eq. 9)}$$

$$\frac{d}{dt}i_{sq} = -\omega_e i_{sd} + \left(-\frac{R_s}{\sigma L_s} - \frac{L_m^2}{\sigma L_s L_r \tau_r}\right)i_{sq} - \frac{L_m}{\sigma L_s L_r}\omega_r\psi_{rd} + \frac{L_m}{\sigma L_s L_r \tau_r}\psi_{rq} + \frac{1}{\sigma L_s}V_{sq} \textit{(Eq.10)}$$

$$\frac{d}{dt}\psi_{rd} = \frac{R_r}{L_r}L_m i_{sd} - \frac{R_r}{L_r}\psi_{rd} + (\omega_e - \omega_r)\psi_{rq} \qquad \textit{(Eq. 11)}$$

$$\frac{d}{dt}\psi_{rq} = \frac{R_r}{L_r}L_m i_{sq} - (\omega_e - \omega_r)\psi_{rd} - \frac{R_r}{L_r}\psi_{rq} \quad \textit{(Eq. 12)}$$

with, $\sigma = \frac{L_s L_r - L_m^2}{L_s L_r}$ and $\tau_r = \frac{L_r}{R_r}$ and rotor speed equation $\frac{d}{dt}\omega_r = \frac{T_e - T_i}{J}$:

While the mechanical equation of a motor that has a polar p-tide. In this case, electromagnetic torque T_e expressed by,

$$T_e = p\left(\frac{L_m}{L_r}\right)\left(i_{s\beta}\psi_{r\alpha} - i_{s\alpha}\psi_{\beta}\right) \quad \textit{(Eq.13)}$$

$$T_e = p\left(\frac{L_m}{L_r}\right)\left(i_{sq}\psi_{rd} - i_{sd}\psi_{q}\right) \quad \textit{(Eq. 14)}$$

The parameters used are as follows:

R_r = Resistance on the rotor (Ω)
R_s = Resistance on the stator (Ω)
L_m= Magnetic inductance (H)
L_s= Magnetic inductance (H)
L_r= Magnetic inductance (H)
σ = Leakage Coefficient
$i_{s\alpha}$ = α axis stator current (A)
$i_{s\beta}$ = β axis stator current (A)
i_{sd} = d-axis stator current(A)
i_{sq} = stator current q axis (A)
T_e = Electromagnetic torque (Nm)
T_l = Load torque (Nm)
$V_{s\alpha}$= Stator voltage on α axis (V)
$V_{s\alpha}$= Stator voltage on the β axis (V)
V_{sd}= Stator voltage on the d-axis (V)
V_{sq}= Stator voltage on the q-axis(V)
$\psi_{r\alpha}$ = Flux of α-axis rotor (Wb)
$\psi_{r\beta}$ = Flux of β-axis rotor (Wb)
ψ_{rd} = d-axis rotor flux (Wb)
ψ_{rq} = q-axis rotor flux (Wb)
ω_r = Rotor velocity (rad/s)
ω_e = Rotating field speed (rad/s)
p = number of poles or poles
τ_r = Rotor constant time

C. *Rotor Field Oriented Control* (RFOC)

The orientation of the FOC (Field Oriented Control) control used has three frames of reference, named the rotor-stator and the air gap. RFOC not require additional processes to separate the interrelationships of variables in the equation. Rotor-oriented FOC (RFOC) can separate (declutch) flux and torque components so that they can be controlled by d-axis stator current (i_{sd}) and q-axis stator current (i_{sq}) respectively. The separation of the two components U_{sd} and U_{sq} is a linear part of the stator voltage after the decoupling process. V_{cd} and V_{cq} are the non-linear part of the stator voltage after the decoupling process is carried out, as follows

$$U_{sd} = R_s i_{sd} + L_s \sigma \frac{d}{dt} i_{sd} \quad \textit{(Eq. 15)}$$

$$U_{sq} = R_s i_{sq} + L_s \sigma \frac{d}{dt} i_{sq} \quad \textit{(Eq. 16)}$$

$$V_{cd} = -\sigma L_s \omega_e i_{sq} + \frac{L_m}{L_r} \frac{d}{dt} \psi_{rd} \quad \textit{(Eq. 17)}$$

$$V_{cq} = \sigma L_s \omega_e i_{sd} + \frac{L_m}{L_r} \omega_e \psi_{rd} \quad \textit{(Eq. 18)}$$

Then the current controller model is modeled as follows:

$$v_{sd}^* = -k_{idp} i_{sd} + k_{idp} i_{sd}^* + k_{idi} x_{sd} - \sigma L_s N \omega_m i_{sq1}^* - \sigma L_s \frac{R_r}{L_r} \frac{{i_{sq1}^*}^2}{i_{sd2}^*} \quad \textit{(Eq. 19)}$$

$$v_{sq}^* = -k_{iqp} i_{sq} + k_{iqp} i_{sq}^* + k_{iqi} x_{sq} + \sigma L_s N \omega_m i_{sd1}^* + \sigma L_s \frac{R_r}{L_r} \frac{i_{sd1}^* {i_{sq1}^*}^2}{i_{sd2}^*} + (1-\sigma) L_s N \omega_m i_{sd2}^* + \frac{(1-\sigma) L_s R_r}{L_r} i_{sq1}^* \quad \text{(Eq. 20)}$$

Where $k_{idp} = \frac{\sigma L_s}{T_d}$, $k_{idi} = \frac{R_s}{T_d}$, $k_{iqp} = \frac{\sigma L_s}{T_d}$, $k_{iqi} = \frac{R_s}{T_d}$

Further, the first order of the reference current of the slip frequency and decoupling calculation becomes,

$$\frac{d}{dt} i_{sd1}^* = \frac{1}{T_d} i_{sd}^* - \frac{1}{T_d} i_{sd1}^* \quad \textit{(Eq. 21)}$$

$$\frac{d}{dt} i_{sq1}^* = \frac{1}{T_d} i_{sq}^* - \frac{1}{T_d} i_{sq1}^* \quad \textit{(Eq. 22)}$$

$$\frac{d}{dt} i_{sd2}^* = \frac{1}{T_2} i_{sd}^* - \frac{1}{T_2} i_{sd2}^* \quad \textit{(Eq.23)}$$

D. MTPA Modelling

The process of the Maximum Torque Per Ampere Method in the MTPA condition process identified for a particular motor torque, the stator current components used are i_d and i_q. MTPA is operated under the condition of each d and q axis flux component in a synchronous reference frame using equations [5]. The Maximum Torque Per Ampere method is shown in Fig 1.

International Journal of Applied Sciences and Smart Technologies
Volume 6, Issue 1, pages 1–9
p-ISSN 2655-8564, e-ISSN 2685-9432

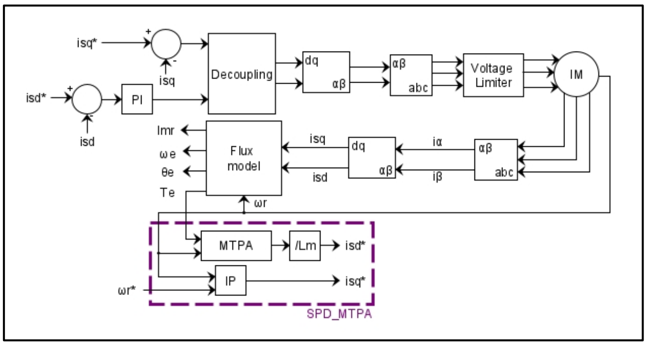

Figure 1. Block Process Diagram MTPA Method

The component values of the d and q axes for the flux synchronous reference frame for the MTPA method are given by the equation.

$$\psi_{ds}|_{TMPA} = \frac{L_s}{L_m}\sqrt{\frac{2T_e L_r}{P}} \tag{Eq. 24}$$

$$\psi_{qs}|_{TMPA} = \frac{\sigma L_s}{L_m}\sqrt{\frac{2T_e L_r}{P}} \tag{Eq. 25}$$

The values of the total flux components on the d and q axes in the synchronous reference frame are shown as

$$|\overrightarrow{\psi_s}|_{TMPA} = \frac{L_s}{L_m}\sqrt{\frac{2L_r\,(1+\sigma^2)T_e}{P}} \tag{Eq. 26}$$

Then substitute $\omega_{sl} = \frac{R_r}{L_r}\frac{i^*_{sq1}}{i^*_{sd2}}$, $v_{sd} = v^*_{sd}$, and $v_{sq} = v^*_{sq}$, $|\psi_s| = \frac{L_s}{L_m}\sqrt{\frac{2L_r(1+\sigma^2)i^*_{sq}}{P}}$ so $i^*_{sd} = 1 + \frac{L_s}{L_m^2}\sqrt{\frac{2L_r(1+\sigma^2)i^*_{sq}}{P}}$

The modeling results that have been linearized into,

$$\begin{aligned}
\frac{d}{dt}\Delta i_{sd} = {} & \left(-\frac{k_{idp}+R_s}{\sigma L_s} - \frac{R_r(1-\sigma)}{\sigma L_r}\right)\Delta i_{sd} + \left(N\omega_{m0} + \frac{R_r i^*_{sq10}}{L_r i^*_{sd20}}\right)\Delta i_{sq} + \left(\frac{L_m R_r}{\sigma L_s L_r^2}\right)\Delta\psi_{rd} + \left(\frac{N L_m \omega_{m0}}{\sigma L_s L_r}\right)\Delta\psi_{rq} + \\
& \left(\frac{k_{idi}}{\sigma L_s}\right)\Delta x_{sd} + \left(\frac{R_r i_{sq0}}{L_r i^*_{sd20}} - \frac{2R_r i^*_{sq10}}{L_r i^*_{sd20}} - N\omega_{m0}\right)\Delta i^*_{sq1} + \left(-\frac{R_r i_{sq0} i^*_{sq10}}{L_r {i^*_{sd20}}^2} + \frac{R_r {i^*_{sq10}}^2}{L_r {i^*_{sd20}}^2}\right)\Delta i^*_{sd2} + \\
& \left(\frac{1}{2}\frac{k_{idp}}{\sigma L_m^2}\left(\frac{2L_r(1+\sigma^2)i^*_{sq0}}{P}\right)^{-\frac{1}{2}}\right)\Delta i^*_{sq} + \left(N i_{sq0} + \frac{N L_m \psi_{rq0}}{\sigma L_s L_r} - N i^*_{sq10}\right)\Delta\omega_m
\end{aligned} \tag{Eq. 27}$$

$$\begin{aligned}
\frac{d}{dt}\Delta i_{sq} = {} & \left(-N\omega_{m0} - \frac{R_r i^*_{sq10}}{L_r i^*_{sd20}}\right)\Delta i_{sd} + \left(-\frac{k_{iqp}+R_s}{\sigma L_s} - \frac{R_r(1-\sigma)}{\sigma L_r}\right)\Delta i_{sq} + \left(-\frac{N L_m \omega_{m0}}{\sigma L_s L_r}\right)\Delta\psi_{rd} + \left(\frac{L_m R_r}{\sigma L_s L_r^2}\right)\Delta\psi_{rq} + \\
& \left(\frac{k_{iqi}}{\sigma L_s}\right)\Delta x_{sq} + \left(N\omega_{m0} + \frac{R_r}{L_r}\frac{i^*_{sq10}}{i^*_{sd20}}\right)\Delta i^*_{sd1} + \left(-\frac{R_r}{L_r}\frac{i_{sd0}}{i^*_{sd20}} + \frac{(1-\sigma)R_r}{\sigma L_r} + \frac{R_r}{L_r}\frac{i^*_{sd10}}{i^*_{sd20}}\right)\Delta i^*_{sq1} +
\end{aligned}$$

International Journal of Applied Sciences and Smart Technologies
Volume 6, Issue 1, pages 1–9
p-ISSN 2655-8564, e-ISSN 2685-9432

$$\left(\frac{R_r}{L_r}\frac{i_{sd0}i^*_{sq10}}{{i^*_{sd20}}^2} - \frac{R_r}{L_r}\frac{i^*_{sd10}i^*_{sq10}}{{i^*_{sd20}}^2} + \left(\frac{(1-\sigma)N\omega_{m0}}{\sigma}\right)\right)\Delta i^*_{sd2} + \left(\frac{k_{iqp}}{\sigma L_s}\right)\Delta i^*_{sq} + \left(-Ni_{sd0} + Ni^*_{sd0} - \frac{NL_m\psi_{rd0}}{\sigma L_s L_r} + \frac{(1-\sigma)Ni^*_{sd20}}{\sigma}\right)\Delta\omega_m \qquad \textit{(Eq. 28)}$$

$$\frac{d}{dt}\Delta\psi_{rd} = \left(\frac{L_mR_r}{L_r}\right)\Delta i_{sd} + \left(-\frac{R_r}{L_r}\right)\Delta\psi_{rd} + \left(\frac{R_r}{L_r}\frac{i^*_{sq10}}{i^*_{sd20}}\right)\Delta\psi_{rq} + \left(\frac{R_r}{L_r}\frac{\psi_{rq0}}{i^*_{sd20}}\right)\Delta i_{sq1} + \left(-\frac{R_r}{L_r}\frac{i^*_{sq10}\,\psi_{rq0}}{{i^*_{sd20}}^2}\right)\Delta i^*_{sd2} \qquad \textit{(Eq. 29)}$$

$$\frac{d}{dt}\Delta\psi_{rq} = \left(\frac{L_mR_r}{L_r}\right)\Delta i_{sq} + \left(\frac{R_r}{L_r}\frac{i^*_{sq10}}{i^*_{sd20}}\right)\Delta\psi_{rd} + \left(-\frac{R_r}{L_r}\right)\Delta\psi_{rq} + \left(-\frac{R_r}{L_r}\frac{\psi_{rq0}}{i^*_{sd20}}\right)\Delta i_{sq1} + \left(\frac{R_r}{L_r}\frac{i^*_{sq10}\,\psi_{rd0}}{{i^*_{sd20}}^2}\right)\Delta i^*_{sd2} \qquad \textit{(Eq. 30)}$$

$$\frac{d}{dt}\Delta\omega_m = \left(-\frac{NL_m\psi_{rq0}}{JL_r}\right)\Delta i_{sd} + \left(\frac{NL_m\psi_{rd0}}{JL_r}\right)\Delta i_{sq} + \left(\frac{NL_m i_{sq0}}{JL_r}\right)\Delta\psi_{rd} + \left(-\frac{NL_m i_{sd0}}{JL_r}\right)\Delta\psi_{rq} + \left(-\frac{1}{J}\right)\Delta T_L \qquad \textit{(Eq. 31)}$$

$$\frac{d}{dt}\Delta x_{sd} = [-1]\Delta i_{sd} + \left(\frac{1}{2}\frac{L_s}{L_m^2}\left(\frac{2L_r(1+\sigma^2)i^*_{sq0}}{P}\right)^{-\frac{1}{2}}\right)\Delta i^*_{sq} \qquad \textit{(Eq. 32)}$$

$$\frac{d}{dt}\Delta x_{sq} = [-1]\Delta i_{sq} + [1]\Delta i^*_{sq} \qquad \textit{(Eq. 33)}$$

$$\frac{d}{dt}\Delta i^*_{sd1} = \left[-\frac{1}{T_d}\right]\Delta i^*_{sd1} + \left[\frac{1}{T_d}\right]\left(\frac{1}{2}\frac{L_s}{L_m^2}\left(\frac{2L_r(1+\sigma^2)i^*_{sq0}}{P}\right)^{-\frac{1}{2}}\right)\Delta i^*_{sq} \qquad \textit{(Eq. 34)}$$

$$\frac{d}{dt}\Delta i^*_{sq1} = \left[-\frac{1}{T_d}\right]\Delta i^*_{sq1} + \left[\frac{1}{T_d}\right]\Delta i^*_{sq} \qquad \textit{(Eq. 35)}$$

$$\frac{d}{dt}\Delta i^*_{sd2} = \left[-\frac{1}{T_2}\right]\Delta i^*_{sd2} + \left[\frac{1}{T_2}\right]\left(\frac{1}{2}\frac{L_s}{L_m^2}\left(\frac{2L_r(1+\sigma^2)i^*_{sq0}}{P}\right)^{-\frac{1}{2}}\right)\Delta i^*_{sq} \qquad \textit{(Eq. 36)}$$

With the equilibrium point as shown by $\omega_{m0} = 209.4254, i^*_{sd0} = 1,\ i^*_{sq0}$ =0.23914

3 Results and Discussions

The induction motor used in this modeling uses an induction motor with specifications, namely a three-phase induction motor, 750 W, 1410 rpm, and 4 poles.

Table 1. Parameters of Induction Motor

Parameter	Symbol	Value
Pole pairs	P	2
Stator Resistance	R_s	2.76 Ω
Rotor Resistance	R_r	2.9 Ω
Stator Inductance	L_s	0.2349 H
Rotor Inductance	L_r	0.2349 H
Mutual Inductance	L_m	0.2279 H

The controller parameters used in the simulation process of each method are shown in Table 1-2.

International Journal of Applied Sciences and Smart Technologies
Volume 6, Issue 1, pages 1–9
p-ISSN 2655-8564, e-ISSN 2685-9432

Table 2. Controller Parameters

Parameter	Symbol	Value
Kp Speed Controler	Kp	0.9
Ki Speed Controler	Ki	0.2

Modeling test by providing several reference speed inputs at 2600 rpm and 3000 rpm.

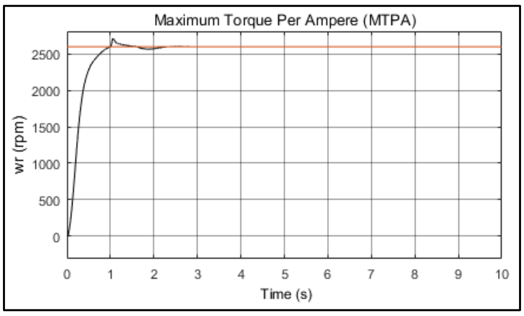

Figure 2. MTPA at 2600 rpm

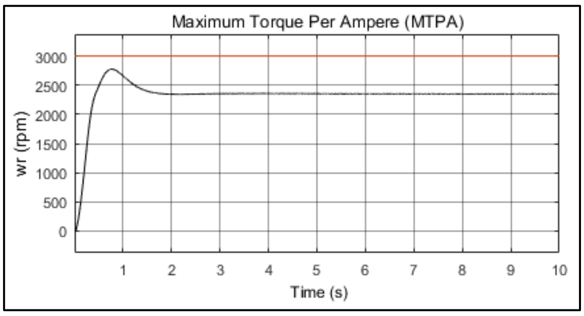

Figure 3. MTPA at 3000 rpm

a. Testing with 2600 rpm speed reference

The test was carried out by providing a reference of 2600 rpm. The response of the system is shown in Fig 2. The response of the system can follow its reference speed, in simulations, there are overshoots and several oscillations, and the time required to reach a steady state. However, the system can reach a steady-state state.

b. Testing with reference speed 3000 rpm.

The test was carried out by providing a reference of 3000 rpm. The response of the system is shown in Fig 3. The response of the system cannot follow the reference speed, because the desired speed has exceeded the speed limit of the system. The system will only stay in the steady-state position even if it not reach its target speed.

4 Conclusions

Studies on modeling with the Maximum Torque Per Ampere (MTPA) Method have been presented. The result of the modeling is that increasing the speed of each different reference input will affect settling time. The higher the speed, the longer it takes for the system to reach a steady-state state. The maximum speed that can be achieved is at a speed of 2600 rpm, so the MTPA method can increase the performance of three-phase induction motors by 84.4%. The above research is limited to the induction motor used is a squirrel cage type three-phase induction motor, and the system uses a speed sensor. The next research direction is to prove the stability of the system by analyzing pole position and movement with variations of Kp, Ki, and Kd and combining the MTPA method with other methods to improve the performance of the induction motor.

Acknowledgements

The writer expresses her thanks to God who always blessed her and to author's family for every support that writers get. Thank you also to the thesis supervisor who has guided and supported writer in the process of writing this journal.

References

[1]. A. Budiarto and O. Judianto, Perancangan Mobil Listrik Ramah Lingkungan Berbasis City Car, Jurnal Inosains Vol. 14 No. 2,2009, pp 38-43.

[2]. Fauzi R, Khair J. Pemodelan Direct Quadrate (DQ) Pada Kendali Kecepatan Motor Induksi Tiga Phasa dengan Field Oriented Control (FOC) Berbasis Kendali PI. ScientiCO: Computer Science and Informatics Journal,2018, pp. 25-35

[3]. H. Setiana, F. Husnayain and F. Yusivar, "Speed Sensorless Control of Dual Induction Motor using Direct Torque Control - Space Vector Modulation," *2019 IEEE 2nd International Conference on Power and Energy Applications (ICPEA)*, Singapore, 2019, pp. 110-114, doi: 10.1109/ICPEA.2019.8818504.

[4]. F. Hamada, F. Husnayain and F. Yusivar, "Speed Sensorless Vector Control of Parallel Connected Induction Motor with Anti-windup Integral-Proportional Speed Controller," 2019 IEEE 2nd International Conference on Power and Energy Applications (ICPEA), Singapore, 2019, pp. 89-93, doi: 10.1109/ICPEA.2019.8818527.

[5]. P. Naganathan and S. Srinivas, "Maximum Torque Per Ampere Based Direct Torque Control Scheme of IM Drive for Electrical Vehicle Applications," 2018 IEEE 18th International Power Electronics and Motion Control Conference (PEMC), Budapest, Hungary, 2018, pp. 256-261, doi: 10.1109/EPEPEMC.2018.8521987.